Nonlinear analysis of reinforced concrete frame under lateral load

Amir Salihovic[*] and Naida Ademovic[a]

Faculty of Civil Engineering at University of Sarajevo,
Patriotske lige 30, 71000 Sarajevo, Bosnia and Herzegovina

Abstract. This study aims to investigate the capacity of different models to reproduce the nonlinear behavior of reinforced concrete framed structures. To accomplish this goal, a combined experimental and analytical research program was carried out on a large scaled reinforced concrete frame. Analyses were performed by SAP2000 and compared to experimental and VecTor2 results. Models made in SAP2000 differ in the simulation of the plasticity and the type of the frame elements used to discretize the frame structure. The results obtained allow a better understanding of the characteristics of all numerical models, helping the users to choose the best approach to perform nonlinear analysis.

Keywords: nonlinear analysis; pushover analysis; frame structure; experimental testing; numerical model; SAP2000; hinges properties

1. Introduction

The most accurate analysis procedure for structures subjected to strong ground motions is the time-history analysis. The pushover analysis is less onerous than nonlinear dynamic analysis since it does not require the monitoring of cyclic inelastic response of structural members and it avoids the dependence on the input motion (Landi *et al.* 2014). The necessity for faster methods that would ensure a reliable structural assessment or design of structures subjected to seismic loading led to the pushover analysis (Themelis 2008).

Pushover is a static nonlinear analysis method where a structure is subjected to gravity loading and a monotonic displacement-controlled lateral load which continuously increases until an ultimate condition is reached (Computers & Structures, Inc. 2016). This analysis can provide a significant insight into the weak links in seismic performance of a structure. A series of iterations are usually required during which, the structural deficiencies observed in one iteration, are rectified and followed by another. This iterative analysis and design process continues until the design satisfies a pre-established performance criterion (Anand and Saravanan 2016). It is assumed that the dynamic response of the building is governed mostly by the first eigen-mode, reducing the problem to a single degree of freedom system. This method enables to track the yielding sequences
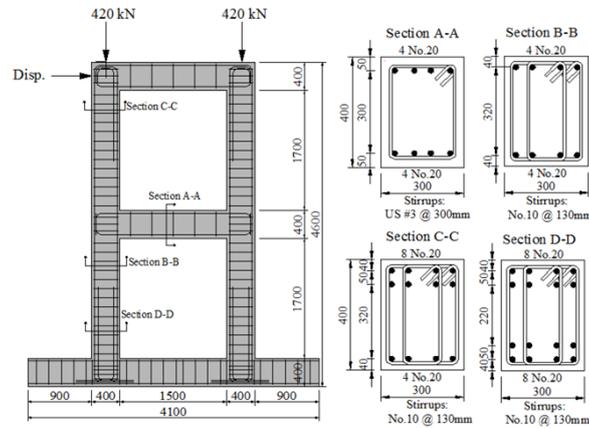

Fig. 1 Frame loads and cross-sections (Güner 2008)

as well as the progress of the overall capacity curve of the structure. Previously elements that have to be defined are the lateral load and its distribution pattern. Once this is defined the lateral load is applied on the numerical model and the amplitude is increased in a stepwise fashion. At each step a nonlinear static analysis is conducted, until the structure becomes unstable or until it reaches a specific limit that has been previously stated (Ademovic *et al*. 2013).

Output generates a static-pushover curve which plots an applied lateral load against displacement. Value of the lateral force incrementally increases and with transition of structure in the nonlinear zone, plastic hinges are formed. When analyzing frame structures, material nonlinearity is assigned to discrete hinge locations where plastic rotation occurs according to FEMA 356 (Federal Emergency Management Agency 2000), ACT-40 (Applied Technology Council 1996) or other set of code-based or user-defined criteria.

The data collected from the experimental testing on the reinforced concrete frame (Duong 2006) provided an extensive database to improve models of structures using different software. Modelling of the tested RC frame was done using two software packages: VecTor2 (Wong *et al*. 2013) and SAP2000 (Computers & Structures, Inc. 2016). Comparison of experimental results with the results obtained in two different software represents the core of this study. Modelling in SAP 2000, was chosen, as it is widely spread and used software in the engineering community, capable to predict nonlinear behavior of frame structures with acceptable accuracy.

2. Experimental program

An experimental program of reinforced concrete frame (Duong 2006) was carried out at the University of Toronto to investigate its behavior under seismic loading conditions. The characteristics of the test frame mimicked, where possible, those of the cement tower located in El Salvador, which is in the one of the world most seismic active areas.

The experiment involved testing of a one-bay, two-storey frame under increasing lateral load levels applied at the second storey beam. Two 420 kN axial column forces were applied to simulate the effects of loads coming from the storeys above the second floor. The experiment consisted of two phases. In Phase A, the frame was laterally loaded until significant damage took

Table 1 Material properties of the frame (Güner 2008)

	Reinforcement								Concrete				
	A_s	d_b	f_y	f_u	E_s	E_{sh}	ε_{sh}	ε_u	f'_c	ε_0	E_c	G_c	μ
	(mm^2)	(mm)	(MPa)	(MPa)	(MPa)	(MPa)	(x10^{-3})	(x10^{-3})	(MPa)	(x10^{-3})	(MPa)	(MPa)	
No.20	300	19.5	447	603	198400	1372	17.1	130.8	42.9	2.31	30058	13069*	0.2*
No.10	100	11.3	455	583	192400	1195	22.8	129.9				* estimated	
US#3	71	11.3	506	615	210000	1025	28.3	134.6					

place in the sections and then was unloaded completely. The frame was then loaded in the reverse direction to the same displacement attained in the forward cycle. The frame was finally unloaded. In Phase B testing, the damaged frame was repaired and then tested under reversed cyclic loading conditions (Güner 2008). The subject of this study is Phase A and state of the tested frame before repairing.

Fig. 1 provides the data regarding the geometrical characteristics of the frame structure that was investigated, as well the reinforcement detailing of the structure.

Where:

A_s - area of tensile longitudinal steel reinforcement;

d_b - diameter of rebar bar;

f_y - yield stress of steel reinforcement;

f_u - ultimate stress of steel reinforcement

E_s - initial elastic modulus of steel;

E_{sh} - hardening elastic modulus of steel;

ε_{sh} - tensile strain in hardening state;

ε_u - tensile strain in ultimate state;

f'_c - specified compressive strength of concrete;

ε_0 - strain at compressive strength of concrete;

E_c - modulus of elasticity of concrete (initial tangent stiffness);

G_c - shear modulus of concrete;

μ - Poisson's ratio;

Material properties used in the frame are presented in Table 1.

Results of the experimental program on the test specimen are represented on a diagram lateral load-displacement (see Fig. 2). In the forward half-cycle of Phase A, the maximum lateral load obtained was approximately 327 kN with a corresponding average top storey lateral displacement of 44,7 mm, as it can be clearly seen in Fig. 2.

A simplified diagram lateral load-displacement (see Fig. 3) is utilized, as this enables an easier comparison between experimental and numerical models. In this simplified diagram the hysteresis curve is represented with 11 key load stages. This data was imported in Excel file and graphically presented by charts and then compared with results from models.

3. Numerical models

3.1 VecTor2

Duong (Duong 2006) modeled the test specimen using VecTor2, a software developed at the University of Toronto. VecTor2 is a program based on the Modified Compression Field Theory
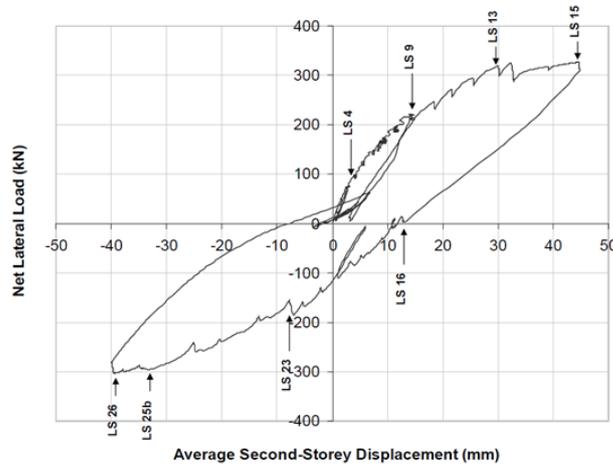
Fig. 2 Lateral load vs. second story displacement - Phase A (Duong 2006)

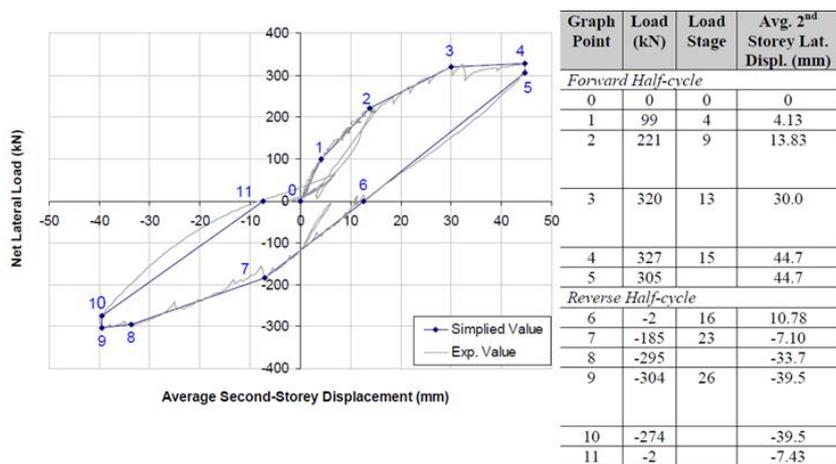| Graph Point	Load (kN)	Load Stage	Avg. 2nd Storey Lat. Displ. (mm)
Forward Half-cycle			
0	0	0	0
1	99	4	4.13
2	221	9	13.83
3	320	13	30.0
4	327	15	44.7
5	305		44.7
Reverse Half-cycle			
6	-2	16	10.78
7	-185	23	-7.10
8	-295		-33.7
9	-304	26	-39.5
10	-274		-39.5
11	-2		-7.43

Fig. 3 Simplified diagram and key load stages of test (Duong 2006)

(MCFT) for nonlinear finite element (FE) analysis of reinforced concrete membrane structures.

The Modified Compression Field Theory was developed by Vecchio and Collins. This theory is capable of predicting the response of reinforced concrete elements to in-plane shear and axial stresses taking into account equilibrium conditions, compatibility requirements, and stress-strain relationships, all expressed in terms of average stresses and average strains. Important aspect is that constitutive relationships for cracked concrete are incorporated for principal compressive stress-principal compressive strain response, as well as for principle tensile stress-principal tensile strain response (Vecchio and Collins 1986). The key simplifying assumption is that the principal strain directions coincides with the principal stress directions. Schematic representation of the theory is illustrated in Fig. 4. The constitutive relations behind the MCFT were derived from the experimental testing of thirty reinforced concrete panels subjected to pure shear or in combination of shear and axial loads.

This theory has been reconfirmed by numerous experimental investigations and analyzed by

many authors (Park 1999, Stevens *et al.* 1987, Bhide and Collins 1989, Vecchio and Nieto 1991a, Vecchio and Nieto 1991b). In all the cases, MCFT was able to predict in a very accurate manner several phenomena: deformations, reinforcement stresses, the behavior in terms of crack patterns, ultimate strengths and failure modes.

The frame was modeled using rectangular elements for modelling concrete while truss elements were used for steel. The author paid attention to fine details in modelling so that the modelling results would be as close as possible to the experimental and analytical results. One example of such detailing is the fact that the base of the specimen was built integrally with the body of the frame and post-tensioned to the strong floor prior to testing. These posttensioning forces were accounted for in the FE modelling by applying six 71 kN downwards forces at the bolt locations (Duong 2006). However, this kind of modelling is time consuming.

It is clear from the Fig. 5 that the obtained value of the peak load in the software VecTor2 is 371 kN. On the other hand, the obtained value from the experiment is lower and reads 327 kN. In this respect it is obvious that by this modeling technique the strength of the frame is overestimated for 12%, which is not negligible.
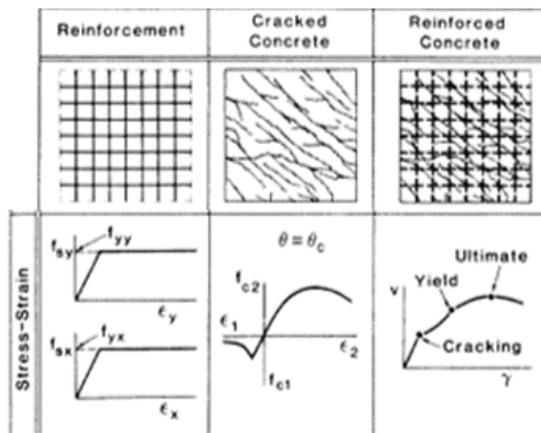

Fig. 4 The Modified compression filed theory for membrane elements (Vecchio and Collins 1986)
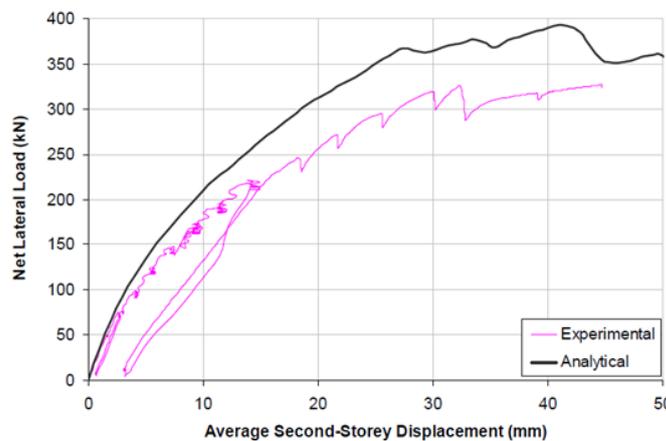

Fig. 5 Phase A Forward Half-Cycle: Lateral Load vs. Second-Storey Displacement (Duong 2006)

Table 2 FEMA Table 6-7 for defining hinge properties of reinforced concrete beams hinges

Table 6-7			Modeling Parameters and Numerical Acceptance Criteria for Nonlinear Procedures-Reinforced Concrete Beams							
			Modeling Parameters			Acceptance Criteria				
						Plastic Rotation Angle, radians				
							Performance level			
Conditions			Plastic Rotation Angle, radians		Residual Strength Ratio			Component Type		
						IO	Primary		Secondary	
			a	b	c		LS	CP	LS	CP
i Beams controlled by flexure[1]										
$\dfrac{\rho - \rho'}{\rho_{bal}}$	Trans Reinf.	$\dfrac{V}{b_w d \sqrt{f'_c}}$								
≤ 0.0	C	≤ 3	0.025	0.05	0.2	0.010	0.02	0.025	0.02	0.05
≤ 0.0	C	≥ 6	0.02	0.04	0.2	0.005	0.01	0.02	0.02	0.04
≥ 0.5	C	≤ 3	0.02	0.03	0.2	0.005	0.01	0.02	0.02	0.03
≥ 0.5	C	≥ 6	0.015	0.02	0.2	0.005	0.005	0.015	0.015	0.02
≤ 0.0	NC	≤ 3	0.02	0.03	0.2	0.005	0.01	0.02	0.02	0.03
≤ 0.0	NC	≥ 6	0.01	0.015	0.2	0.0015	0.005	0.01	0.01	0.015
≥ 0.5	NC	≤ 3	0.01	0.015	0.2	0.005	0.01	0.01	0.01	0.015
≥ 0.5	NC	≥ 6	0.005	0.01	0.2	0.0015	0.005	0.005	0.005	0.01

Table 3 FEMA Table 6-8 for defining hinge properties of reinforced concrete columns hinges

Table 6-8			Modeling Parameters and Numerical Acceptance Criteria for Nonlinear Procedures-Reinforced Concrete Columns							
			Modeling Parameters			Acceptance Criteria				
						Plastic Rotation Angle, radians				
							Performance level			
Conditions			Plastic Rotation Angle, radians		Residual Strength Ratio			Component Type		
						IO	Primary		Secondary	
			a	b	c		LS	CP	LS	CP
i Columns controlled by flexure[1]										
$\dfrac{P}{A_g f'_c}$	Trans Reinf.	$\dfrac{V}{b_w d \sqrt{f'_c}}$								
≤ 0.1	C	≤ 3	0.02	0.03	0.2	0.005	0.0015	0.02	0.02	0.03
≤ 0.1	C	≥ 6	0.016	0.024	0.2	0.005	0.012	0.016	0.016	0.024
≥ 0.4	C	≤ 3	0.015	0.025	0.2	0.003	0.012	0.015	0.018	0.025
≥ 0.4	C	≥ 6	0.012	0.02	0.2	0.003	0.01	0.012	0.013	0.02
≤ 0.1	NC	≤ 3	0.006	0.015	0.2	0.005	0.005	0.006	0.01	0.015
≤ 0.1	NC	≥ 6	0.005	0.012	0.2	0.005	0.004	0.005	0.008	0.012
≥ 0.4	NC	≤ 3	0.003	0.01	0.2	0.002	0.002	0.003	0.006	0.01
≥ 0.4	NC	≥ 6	0.002	0.008	0.2	0.002	0.002	0.002	0.005	0.008

3.2 Modeling of the frame using the commercial program SAP2000

SAP2000 has proven to be one of the most integrated, productive and practical general purpose structural finite element (FE) program on the market today. It is user-friendly and wide spread program in earthquake engineering today. Modelling of the frame was made with the latest version of SAP2000 19.0.0. Nonlinear behavior in SAP2000, is assumed to occur within the frame elements at the location of the plastic hinges (Nahavandi 2015). A hinge property is a named set of nonlinear properties that can be assigned to points along the length of one or more frame elements.

There are three types of hinge properties in SAP2000 (Computers & Structures, Inc. 2016):
• Automatic hinge properties;
• User-defined hinge properties; and
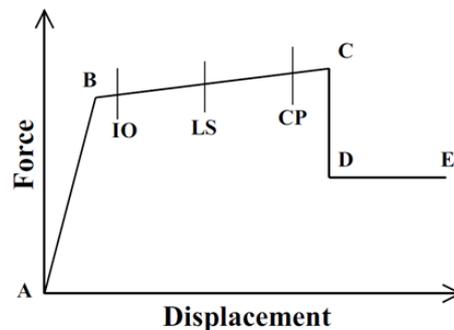• Generated hinge properties.

Fig. 6 Plastic hinge behavior according to FEMA 356 (Computers & Structures, Inc. 2016)

Automatic hinge properties cannot be modified. They also cannot be viewed because the automatic properties are section dependent. The automatic properties cannot be fully defined by the program until the section that they apply to is identified. User-defined hinge properties can be either based on automatic properties or they can be fully user-defined. When user-defined properties are based on automatic properties, the hinge properties cannot be viewed because, again, the automatic properties are section dependent. When user-defined properties are not based on automatic properties, then the properties can be viewed and modified. Only automatic hinge properties and user-defined hinge properties can be assigned to frame elements. Once automatic or user-defined hinge properties are assigned to a frame element, the program automatically creates a generated hinge property for each and every hinge (Computers & Structures, Inc. 2016). The built-in automatic hinge properties for concrete members are based on Tables 6-7 (see Table 2) for beams and 6-8 (see Table 3) for columns in FEMA 356 (Federal Emergency Management Agency 2000).

FEMA 356 documents have developed modelling parameters, acceptance criteria and procedures of pushover analysis. These documents define force-deformation criteria for hinges used in pushover analysis. In Fig. 6 five points are given (A, B, C, D and E), used to define the hinge rotation behavior of RC members and the acceptance criteria on a force versus deformation diagram. Based on the backbone curve presented in Fig. 6 no plastic deformation occurs until point B where the hinge yields. So, the line A-B represent the elastic behavior of the element. This is followed by a yield plateau or strain hardening behavior until point C which represents the ultimate capacity of the hinge.

After point C, the hinge's force capacity immediately drops to point D which corresponds to the residual strength of the hinge. Point E represents the ultimate displacement capacity of the hinge after which the total failure of the hinge is reached at point E. There are three stages marked between point B and C. IO corresponds to immediate occupancy, LS to life safety, and CP to collapse prevention (López-Almansa *et al.* 2014).

Structural performance immediate occupancy (IO) means the post-earthquake damage state in which only very limited structural damage has occurred. Life safety (LS) defines the post-earthquake damage state in which significant damage to the structure has occurred, but some margin against either partial or total structural collapse remains, and collapse prevention (CP) means the building is on the verge of experiencing partial or total collapse (Bansal 2011).

Three models were created in SAP2000. They differ in the simulation of the plasticity and the type of the frame elements used to discretize the frame structure. Lumped and distributed plasticity models were used to define the nonlinear behavior of the structure. The nonlinear behavior in the lumped plasticity model (LP) is concentrated in a number of zero-length plastic hinges, usually located near the connections among the frame elements. The behavior of each plastic hinge is characterized by force-displacement relations which are automatic or user-defined. Moreover, a lumped plasticity/damage model is often used considering inelastic hinges at pre-described locations, placed at both ends of the (elastic) beam. (Jukic *et al.* 2014) Distributed (fiber section) plasticity (DP) models are used to simulate the spread of plasticity along the member length and across the section. This plasticity method discretizes the structural members into many line segments - fibers, and further subdivides the cross-section of each segment into a number of finite elements. (Izadpanaha and Habibi 2015) Each fiber is associated with a uniaxial stress strain relationship, and then the sectional behavior is obtained by integration imposing the Navier-Bernoulli hypothesis (Nahavandi 2015, Belejo *et al*. 2012).

In each model frame elements were used for modelling of the beams and columns and plastic hinges were concentrated at both ends of both elements. Frame rectangular sections were used for the first model while for the other two models the section properties were created with Section Designer. Beams have only moment (M3) hinges, whereas columns have axial load and moment (P-M3) hinges. The moment–rotation relations and the acceptance criteria for the performance levels of the hinges were obtained from FEMA 356 guideline (Federal Emergency Management Agency 2000). Hinges were assigned on 0,05 and 0,95 of the relative distance of each frame element.

3.2.1 Frame sections with user-defined hinges

Resistance of cross-sections of the tested frame was calculated in order to define the plastic hinges behavior. In that regard the moment–rotation relations were calculated with the help of FEMA 356 guideline [4] and specific values of moment and rotation in points B, C, D and E were assigned. Calculation of resistance of section A is shown below.
Cracking moment and curvature

$$M_{cr} = \frac{I}{y_{cg}} \cdot f_{ctm} = \frac{1,6 \cdot 10^{-3}}{0,2} \cdot 2,9 \cdot 10^{3} = 23,2 kNm \tag{1}$$

$$\kappa_{cr} = \frac{M_{cr}}{E_{cm} \cdot I} = \frac{23,2}{3,194 \cdot 10^{7} \cdot 1,6 \cdot 10^{-3}} = 0,000454 \frac{1}{m} \tag{2}$$

Yielding moment and curvature

$$M_y = F_{sy,t} \cdot (d - k \cdot x) = 600 \cdot (0,35 - 0,416 \cdot 0,0968) = 185,84 kNm \tag{3}$$

$$\varepsilon_{sk} = \frac{f_{yk}}{E_{sm}} = \frac{500}{2 \cdot 10^5} = 2,5 \cdot 10^{-3} \tag{4}$$

$$\kappa_y = \frac{\varepsilon_{sk}}{d - x} = \frac{2,5 \cdot 10^{-3}}{0,35 - 0,0968} = 0,00987 \frac{1}{m} \tag{5}$$

Moment-rotation relations

$$\phi_{cr} = \kappa_{cr} \cdot l_p = 0,000454 \cdot 0,40 = 0,0001816 rad \qquad\qquad M_{cr}=23,2 \text{ kNm}$$

$$\phi_y = \kappa_y \cdot l_p = 0,00987 \cdot 0,40 = 0,003948 rad \qquad\qquad M_y=185,84 \text{ kNm}$$

$$\phi_B = \phi_y = 0,003948 rad \qquad\qquad M_B=185,84 \text{ kNm}$$

$$\phi_C = \phi_B + a = 0,028948 rad \qquad\qquad M_C=185,84+0,1 \cdot 185,84=204,42 \text{ kNm}$$

$$\phi_D = \phi_C = 0,028948 rad \qquad\qquad M_D=0,2 \cdot 204,42=40,85 \text{ } kNm$$

$$\phi_E = \phi_B + b = 0,053948 rad \qquad\qquad M_E=M_D=0,2 \cdot 204,42=40,85 \text{ } kNm$$

Where:
Mcr - cracking moment of cross-section;
I - moment of inertia;
ycg - center of gravity;
fctm - mean value of axial tensile strength of concrete;
κcr - cracking curvature;
Ecm - secant modulus of elasticity of concrete;
My - yielding moment of cross-section;
Fsy,t - yield tensile force of steel reinforcement;
d - effective depth of a cross-section;
k – coefficient of compression force position;
x - neutral axis depth;
εsk - characteristic yield tensile strain of reinforcement;
fyk - characteristic yield strength of reinforcement;
Esm - secant modulus of elasticity of steel;
κy - yielding curvature of cross-section;
Φcr - cracking rotation of cross-section;
lp - hinge length;
Φy - yielding rotation of cross-section;
a, b - plastic rotation angle from Table 2 (FEMA 356).
On the beam (Section A-A), as indicated in Fig. 7, the moment (M3) hinge was assigned and plastic hinge properties were defined according to FEMA 356 (see Table 1). Guidelines for hinge
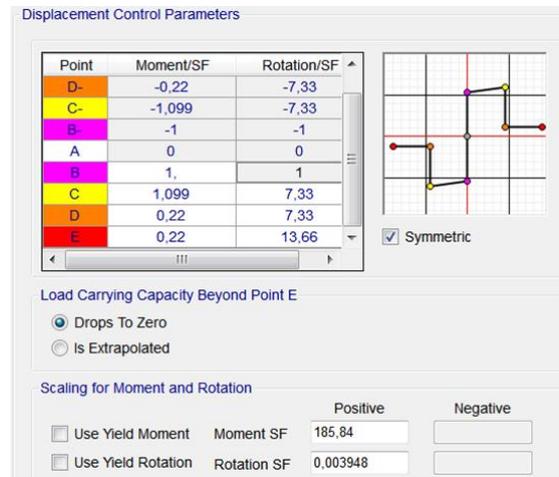
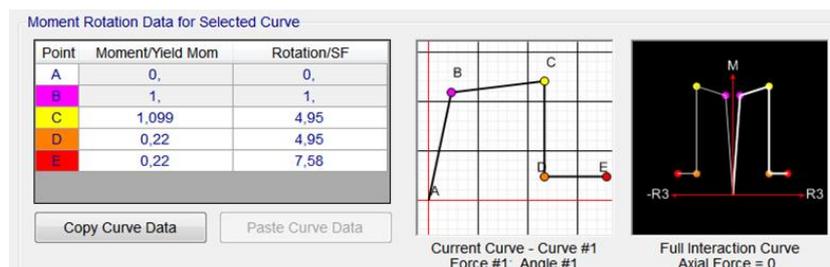Fig. 7 Moment-rotation curve of M3 hinge for Section A-A

Fig. 8 Moment-rotation curve of P-M3 hinge for Section B-B

length are given in FEMA 356 and ASCE 41-13 (American Society of Civil Engineers 2014) and it is selected to be equal to the depth of the cross-section. When defining the hinge moment-rotation curve the values were normalized with respect to the yield moment and yield rotation of the section (scaled factor - SF). In this respect point B represent the starting point with normalized value (1,1) threshold.

Nonlinear behavior of the column sections (Section B-B, C-C and D-D), as illustrated in Fig. 8, was achieved using the interacting axial-moment (P-M3) hinges on both ends of the column. Plastic hinge properties which define moment-rotation relations were calculated according to Table 6-8 for columns in FEMA 356 (see Table 2).

3.2.2 Section designer with auto hinges

Section Designer is a separate utility built into SAP2000 that can be used to create specific frame section properties. It allows sections of arbitrary geometry and combinations of materials to be created. Unlike default frame sections built in SAP2000, which allows the usage of only one main m aterial (concrete), in Section Designer it is possible to create a section with different concrete material properties and precise disposition of rebars.

On the left hand side of the Fig. 9 detail of the reinforcement of the columns is illustrated. This kind of detailing to a certain degree can be modelled by the Section Designer as seen on the right hand side of the Fig. 9. As it can be seen the exact location of the rebars is obtained as well as two
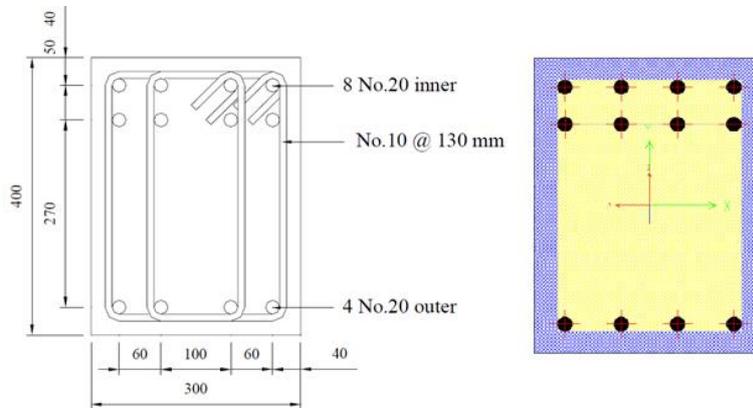
Fig. 9 Section C-C created with Section Designer

| (a) Confined concrete model | (b) Unconfined concrete model |

Fig. 10

different material properties of concrete.Cross-sections were defined in Section Designer with two types of concrete, one which is confined (yellow color) and other unconfined (blue color). Unconfined concrete was assigned for the concrete cover and confined for the rest of the section, with aim to model the frame sections with more accuracy.

Confinement in concrete is achieved by the suitable placement of transverse reinforcement. At low levels of stress, transverse reinforcement is hardly stressed; the concrete behaves much like unconfined concrete. At stresses close to the uniaxial strength of concrete internal fracturing causes the concrete to dilate and bear out against the transverse reinforcement which then causes a confining action in concrete. This phenomenon of confining concrete by suitable arrangement of transverse reinforcement causes a significant increase in the strength and ductility of concrete (Reddiar 2010).

Mander's (Mander *et al*. 1988) concrete model, shown in Fig. 10, was used to model confined and unconfined concrete stress-strain relationships. Mander's concrete stress-strain curve calculates the compressive strength and ultimate strain values as a function of the confinement (transverse reinforcing) steel (Computers & Structures, Inc. 2008).

It should be stated here that when automatic hinge properties are used, the program automatically
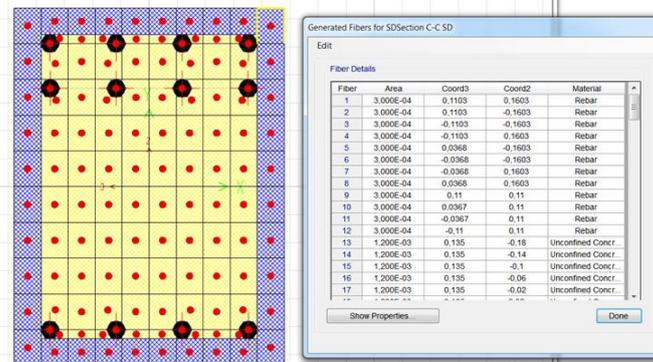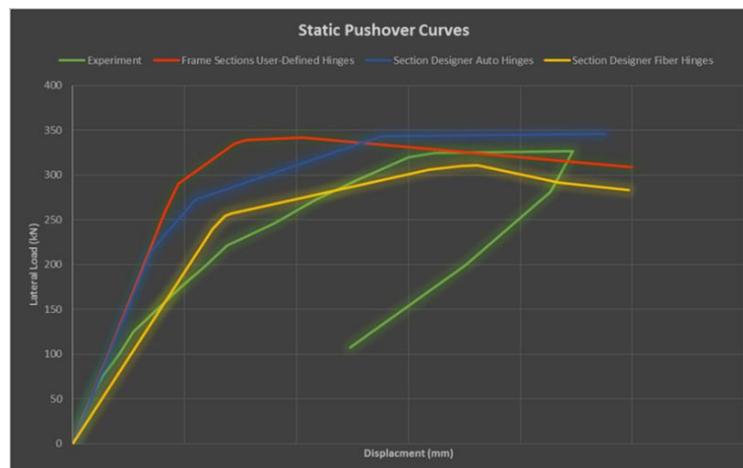
Fig. 11 Section C-C generated fibers

Fig. 12 Static pushover curves: Experimental vs. SAP2000 models

calculates the moment-rotation curve and other hinge properties from the Section Designer characteristics according to FEMA 356 criteria. Section and hinge properties are calculated with high accuracy because of precision of created section in respect of geometry and material properties.

3.2.3 Section designer with fiber hinges

Distributed plasticity models or so-called fiber section models are used to simulate the spread of plasticity along the member length and across the section. Fiber hinges are used to define the coupled axial force and bending behavior at locations along the length of a frame element. The cross section is discretized into a series of representative axial fibers which extend longitudinally along the hinge length. These hinges are elastic-plastic and consist of a set of material points, each representing a portion of the frame cross-section having the same material. Force-deflection and moment-rotation curves are not specified, but rather are computed during the analysis from the stress-strain curves of the material points (Computers & Structures, Inc. 2006).

Depending on the material in its tributary area, each fiber has a stress-strain relationship. Integrating the behavior over the cross section, then multiplying by the hinge length, one obtains the axial force-deformation and biaxial moment-rotation relationships (Botez *et al.* 2014). The section

Table 4 Peak load comparison of different models

	Duong Frame Models	Peak Load (kN)	Difference (%).
	Experimental Program	327 kN	-
	VecTor2	371 kN	+12%
SAP2000	Frame Section User-Defined Hinges	341 kN	+4%
	Section Designer Auto Hinges	347 kN	+7%
	Section Designer Fiber Hinges	311 kN	-5%

stiffness is computed based on the tangent stiffness of each fiber material, on its area of influence and on its coordinates within the cross section (Carvalho *et al*. 2013). The fiber hinge model is more accurate as the nonlinear material relationship of each fiber automatically accounts for interaction, changes along the moment-rotation curve, and plastic axial strain.

Each section was divided into three types of fibers for different kind of materials. There were 12 rebar fibers, 36 unconfined concrete fibers and 80 confined concrete fibers, which makes a total of 128 fibers (see Fig. 11). More fibers mean also more complex calculation requiring more computer storage and execution time. Optimum number of the fibers needs to be found to get an optimum balance between accuracy and computational efficiency.

4. Comparison of results

The pushover analysis was performed in all of the models and compared with the obtained data from the experiments conducted in (Duong 2006). The results obtained through the pushover analysis using three different models in SAP2000 compared to experimental program are shown in the Fig. 12.

From the results obtained it is possible to notice that, in general, the pushover curves from SAP2000 are pretty close to one obtained in experimental program. Both models with lumped plasticity approach (concentrated hinges) overestimated the strength of the frame structure, while the model with distributed plasticity (fiber hinges) underestimated the strength to some extent. The biggest difference is in the initial stiffness, where models with concentrated hinges had a larger value of stiffness, but after that the stiffness declined and pushover curve was closer to one obtained in the experimental program. This can be attributed to the linear-elastic behavior of hinges until yielding, which is in fact a simplification made according to FEMA 356 documents. On the other hand, in fiber-based modelling, the section is discretized in a number of areas (material points), each of which employs its stress-strain curve. Force-deflection relation is computed during the analysis from the stress-strain curves of the material points and as a result there is nonlinearity also in the initial part of pushover curve before yielding. However, if we compare peak load values of all models there is not big difference. In Table 4, shown below, peak loads are compared including also results obtained from the calculations done in VecTor2.

5. Conclusions

A large scaled reinforced concrete frame was experimentally tested by Duong. During the

analysis expected nonlinear response was observed. Different software were used for numerical modeling of the frame structure and then compared. Based on results obtained for different numerical models the following conclusions can be made.

It is interesting to note that if only peak load is taken into account, all models made in SAP2000 are close to experimental program results. However, the overall nonlinear behavior and the shape of the pushover curve obtained in VecTor2 is in an excellent correlation with the experimental data. It is only the SAP2000 model with fiber hinges which is close to it. This can be explained by the influence of the second-order effects (concrete shrinkage, concrete tension stiffening, shear deformation, membrane action) which are taken into account in VecTor2. This all is covered by detailed modelling done in VecTor2, which requires a lot of the time and "expert-level knowledge" to incorporate it into model.

Frame section user-defined hinges and Section Designer auto hinges models (lumped plasticity approach) predicted a slightly greater peak load and higher initial stiffness than the experimental results. User-defined hinges required a lot of calculation before creating a model of the structure and additional effort has to be made. Section Designer has been proved to be powerful tool built in SAP2000. It allows sections of arbitrary geometry and combinations of materials to be created with quite good accuracy which led to good results when using automatically hinges.

The definition of the plastic hinges through fiber elements is the approach that leads to the best pushover results in SAP2000. It is important to find an optimum number of fibers in order to get the best balance between accuracy and computational efficiency. Section Designer auto hinges should be considered as a good alternative for more complex 3D structures since fiber hinge models take a much longer time for calculations.

References

Ademovic, N., Hrasnica, M. and Oliveira, D.V. (2013), "Pushover analysis and failure pattern of a typical masonry residential building in Bosnia and Herzegovina", *Eng. Struct.*, **50**, 13-29.

American Society of Civil Engineers and Structural Engineering Institute (2014), *Seismic Evaluation and Retrofit of Existing Buildings*, American Society of Civil Engineering, Reston, Virginia, U.S.A.

Anand, R. and Saravanan, M.E. (2016), "Non-linear analysis of reinforced concrete framed structure using SAP", *Int. J. Tech. Res. Appl.,* **4**(4), 41-45.

Applied Technology Council (1996), *Seismic Evaluation and Retrofit of Concrete Buildings, Volume 1-2*, Redwood City, California, U.S.A.

Bansal, R. (2011), "Pushover analysis of reinforced concrete frame", M.Sc. Dissertation, Thapar University, Punjab.

Belejo, A., Bento, R. and Bhatt, C. (2012), "Comparison of different computer programmes to predict the seismic performance of the SPEAR building by means of pushover analysis", *Proceedings of the 15th World Conference on Earthquake Engineering*, Lisbon, Portugal, September.

Bhide, S.B. and Collins, M.P. (1989), "Influence of axial tension on the shear capacity of reinforced concrete members", *ACI Struct. J.*, **86**(5), 570-581.

Botez, M.D., Bredean, L.A. and Ioani, A.M. (2014), "Plastic hinge vs. distributed plasticity in the progressive collapse analysis", *Acta Tech. Napocens.: Civil Eng. Architect.*, **57**(1), 24-36.

Carvalho, G., Bento, R. and Bhatt, C. (2013), "Nonlinear static and dynamic analyses of reinforced concrete buildings-comparison of different modelling approaches", *Earthq. Struct.*, **4**(5), 451-470.

Computers & Structures, Inc. (2008), *Technical Note. Material Stress-Strain Curves*, Berkeley, California, U.S.A.

Computers & Structures, Inc. (2016), *CSI Analysis Reference Manual for SAP2000, ETABS, SAFE and*

CSIBridge, Berkeley, California, U.S.A.

Duong, K.V. (2006), "Seismic behaviour of a shear-critical reinforced concrete frame: An experimental and numerical investigation", M.Sc. Dissertation, University of Toronto, Toronto, Canada.

Federal Emergency Management Agency (2000), *Prestandard and Commentary for the Seismic Rehabilitation of Buildings*, Washington, D.C., U.S.A.

Güner, S. (2008), "Performance assessment of shear-critical reinforced concrete plane frames", Ph.D. Dissertation, University of Toronto, Toronto.

Güner, S. and Vecchio, F.J. (2010), "Pushover analysis of shear-critical frames: Formulation", *ACI Struct. J.*, **107**(1), 63-71.

Izadpanaha, M. and Habibi, A. (2015), "Evaluating the spread plasticity model of IDARC for inelastic analysis of reinforced concrete frames", *Struct. Eng. Mech.*, **56**(2), 169-188.

Jukić, M., Brank, B. and Ibrahimbegovic, A. (2014), "Failure analysis of reinforced concrete frames by beam finite element that combines damage, plasticity and embedded discontinuity", *Eng. Struct.*, **75**, 507-527.

Landi, L., Pollio, B. and Diotallevi, P.P. (2014), "Effectiveness of different standard and advanced pushover procedures for regular and irregular RC frames", *Struct. Eng. Mech.*, **51**(3), 433-446.

López-Almansa, F., Alfarah, B. and Oller, S. (2014), "Numerical simulation of RC frame testing with damaged plasticity model. Comparison with simplified models", *Proceedings of the 2nd European Conference on Earthquake Engineering and Seismology*, Istanbul, Turkey, August.

Mander, J.B., Priestley, M.J. and Park, R. (1988), "Theoretical stress-strain model for confined concrete", *J. Struct. Eng.*, **114**(8), 1804-1826.

Nahavandi, H. (2015), "Pushover analysis of retrofitted reinforced concrete buildings", M.Sc. Project Report, Portland State University, Oregon, U.S.A.

Park, S.Y. (1999), "Predictions of shear strength of R/C beams using modified compression field theory and ACI Code", *KCI Concrete J.*, **11**(3), 5-17.

Reddiar, M.K.M. (2010), "Stress-strain model of unconfined and confined concrete and stress-block parameters", M.Sc. Dissertation, Texas A&M University, College Station, Texas, U.S.A.

Stevens, N.J., Uzumeri, S.M. and Collins, M.P. (1987), *Analytical Modelling of Reinforced Concrete Subjected to Monolithic and Reversed Loadings*, Publication 87-1, Department of Civil Engineering, University of Toronto, Toronto, Canada.

Themelis, S. (2008), "Pushover analysis for seismic assessment and design of structures", Ph.D. Dissertation, Heriot-Watt University, Edinburgh, Scotland.

Vecchio, F.J. and Balopoulou, S. (1990), "On the nonlinear behavior of reinforced concrete frames", *Can. J. Civil Eng.*, **17**(5), 698-704.

Vecchio, F.J. and Collins, M.P. (1986), "The modified compression-field theory for reinforced concrete elements subjected to shear", *ACI J.*, **83**(2), 219-231.

Vecchio, F.J. and Nieto, M. (1991), "Reinforced concrete membrane elements with perforations", *ASCE J. Struct. Eng.*, **116**(9), 2344-2360.

Vecchio, F.J. and Nieto, M. (1991), "Shear-friction tests on reinforced concrete panels", *ACI Struct. J.*, **88**(3), 371-379.

Wong, P.S., Vecchio, F.J. and Trommels, H. (2013), *Vector2 & Formworks User's Manual*, 2nd Edition, Texas A & M University.

AI